LUND UNIVERSITY

A Closed Form Expression for the Exact Bit Error Probability for Viterbi Decoding of Convolutional Codes

Bocharova, Irina; Hug, Florian; Johannesson, Rolf; Kudryashov, Boris

Link to publication

A Closed Form Expression for the Exact Bit Error Probability for Viterbi Decoding of Convolutional Codes

Irina E. Bocharova, Florian Hug, *Student Member, IEEE*,
Rolf Johannesson, *Life Fellow, IEEE*, and Boris D. Kudryashov

Abstract—In 1995, Best et al. published a formula for the exact bit error probability for Viterbi decoding of the rate $R = 1/2$, memory $m = 1$ (2-state) convolutional encoder with generator matrix $G(D) = (1 \quad 1 + D)$ when used to communicate over the binary symmetric channel. Their formula was later extended to the rate $R = 1/2$, memory $m = 2$ (4-state) convolutional encoder with generator matrix $G(D) = (1 + D^2 \quad 1 + D + D^2)$ by Lentmaier et al.

In this paper, a different approach to derive the exact bit error probability is described. A general recurrent matrix equation, connecting the average information weight at the current and previous states of a trellis section of the Viterbi decoder, is derived and solved. The general solution of this matrix equation yields a closed form expression for the exact bit error probability. As special cases, the expressions obtained by Best et al. for the 2-state encoder and by Lentmaier et al. for a 4-state encoder are obtained. The closed form expression derived in this paper is evaluated for various realizations of encoders, including rate $R = 1/2$ and $R = 2/3$ encoders, of as many as 16 states.

Moreover, it is shown that it is straightforward to extend the approach to communication over the quantized additive white Gaussian noise channel.

Index Terms—additive white Gaussian noise channel, binary symmetric channel, bit error probability, convolutional code, convolutional encoder, exact bit error probability, Viterbi decoding

I. INTRODUCTION

In 1971, Viterbi [1] published a nowadays classical upper bound on the bit error probability P_{b} for Viterbi decoding, when convolutional codes are used to communicate over the binary symmetric channel (BSC). This bound was derived from the extended path weight enumerators, obtained using a signal flow chart technique for convolutional encoders. Later, van de Meeberg [2] used a very clever observation to tighten Viterbi's bound for large signal-to-noise ratios (SNRs).

The challenging problem of deriving an expression for the *exact* (decoding) bit error probability was first addressed by

Morrissey in 1970 [3] for a suboptimal feedback decoding algorithm. He obtained the same expression for the exact bit error probability for the rate $R = 1/2$, memory $m = 1$ (2-state) convolutional encoder with generator matrix $G(D) = (1 \quad 1 + D)$ that Best et al. [4] obtained for Viterbi decoding. Their method is based on considering a Markov chain of the so-called metric states of the Viterbi decoder; an approach due to Burnashev and Cohn [5]. An extension of this method to the rate $R = 1/2$ memory $m = 2$ (4-state) convolutional encoder with generator matrix $G(D) = (1 + D^2 \quad 1 + D + D^2)$ was published by Lentmaier et al. [6].

In this paper we use a different and more general approach to derive a closed form expression for the exact (decoding) bit error probability for Viterbi decoding of convolutional encoders, when communicating over the BSC as well as the quantized additive white Gaussian noise (AWGN) channel. Our new method allows the calculation of the exact bit error probability for more complex encoders in a wider range of code rates than the methods of [4] and [6]. By considering a random tie-breaking strategy, we average the information weights over the channel noise sequence and the sequence of random decisions based on coin-flippings (where the coin may have more than two sides depending on the code rate). Unlike the backward recursion in [4] and [6], the bit error probability averaged over time is obtained by deriving and solving a recurrent matrix equation for the average information weights at the current and previous states of a trellis section when the maximum-likelihood branches are decided by the Viterbi decoder at the current step.

To illustrate our method, we use a rate $R = 2/3$ systematic convolutional 2-state encoder whose minimal realization is given in observer canonical form, since this encoder is both general and simple.

In Section II, the problem of computing the exact bit error probability is reformulated via the average information weights. A recurrent matrix equation for these average information weights is derived in Section III and solved in Section IV. In Section V, we give additional examples of rate $R = 1/2$ and $R = 2/3$ encoders of various memories. Furthermore, we analyze a rate $R = 1/2$ 4-state encoder used to communicate over the quantized additive white Gaussian noise (AWGN) channel and show an interesting result that would be difficult to obtain without being able to calculate the exact bit error probability.

Before proceeding, we would like to emphasize that the bit error probability is an encoder property, neither a generator matrix property nor a convolutional code property.

II. PROBLEM FORMULATION VIA THE AVERAGE INFORMATION WEIGHTS

Assume that the all-zero sequence is transmitted over a BSC with crossover probability p and let $W_t(\sigma)$ denote the weight of the information sequence corresponding to the code sequence decided by the Viterbi decoder at state σ and time instant t. If the initial values $W_0(\sigma)$ are known, then the random process $W_t(\sigma)$, $t = 0, 1, 2, \ldots$, is a function of the random sequence of the received c-tuples $\boldsymbol{r}_\tau$, $\tau = 0, 1, \ldots, t-1$, and the coin-flippings used to resolve ties.

Our goal is to determine the mathematical expectation of the random variable $W_t(\sigma)$ over this ensemble, since for rate $R = b/c$ minimal convolutional encoders the bit error probability can be computed as the limit

$$P_{\mathrm{b}} = \lim_{t \to \infty} \frac{E\left[W_t(\sigma = 0)\right]}{tb} \tag{1}$$

assuming that this limit exists.

Remark. If we consider nonminimal encoders, all states equivalent to the all-zero state have to be also taken into account.

We consider encoder realizations in both controller and observer canonical form and denote the encoder states by σ, $\sigma \in \{0, 1, \ldots, |\Sigma| - 1\}$, where Σ is the set of all possible encoder states.

During the decoding step at time instant $t+1$ the Viterbi algorithm computes the cumulative Viterbi branch metric vector $\boldsymbol{\mu}_{t+1} = (\mu_{t+1}(0) \ \mu_{t+1}(1) \ldots \mu_{t+1}(|\Sigma| - 1))$ for the time instant $t+1$ using the vector $\boldsymbol{\mu}_t$ and the received c-tuple $\boldsymbol{r}_t$. It is convenient to normalize the metrics such that the cumulative metrics at every all-zero state will be zero, that is, we subtract the value $\mu_t(0)$ from $\mu_t(1), \mu_t(2), \ldots, \mu_t(|\Sigma|-1)$ and introduce the normalized cumulative branch metric vector

$$\boldsymbol{\phi}_t = \left(\phi_t(1) \ \phi_t(2) \ldots \phi_t(|\Sigma| - 1)\right)$$
$$= \left(\mu_t(1) - \mu_t(0) \ \mu_t(2) - \mu_t(0) \ldots \mu_t(|\Sigma| - 1) - \mu_t(0)\right)$$

For example, for a 2-state encoder we obtain the scalar

$$\phi_t = \phi_t(1)$$

while for a 4-state encoder we have the vector

$$\boldsymbol{\phi}_t = \left(\phi_t(1) \ \phi_t(2) \ \phi_t(3)\right)$$

The elements of the random vector $\boldsymbol{\phi}_t$ belong to a set whose cardinality M depends on the channel model, encoder structure, and the tie-breaking rule. Enumerating the vectors $\boldsymbol{\phi}_t$ by numbers ϕ_t which are random variables taking on M different integer values $\phi^{(0)}, \phi^{(1)}, \ldots, \phi^{(M-1)}$, the sequence of numbers ϕ_t forms an M-state Markov chain Φ_t with transition probability matrix $\Phi = (\phi_{jk})$, where

$$\phi_{jk} = \Pr\left(\phi_{t+1} = \phi^{(k)} \,\Big|\, \phi_t = \phi^{(j)}\right) \tag{2}$$

Let $\boldsymbol{W}_t$ be the vector of information weights at time instant t that depends both on the $|\Sigma|$ encoder states σ_t and on the M normalized cumulative metrics ϕ_t; that is, $\boldsymbol{W}_t$ is expressed as the following vector with $M|\Sigma|$ entries

$$\boldsymbol{W}_t = \left(\boldsymbol{W}_t(\sigma = 0) \ \boldsymbol{W}_t(\sigma = 1) \ \ldots \ \boldsymbol{W}_t(\sigma = |\Sigma| - 1)\right) \tag{3}$$
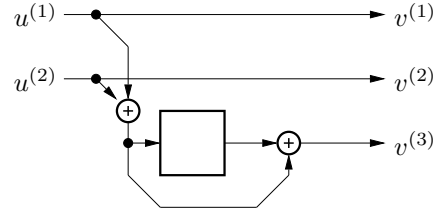

Fig. 1: A minimal encoder for the generator matrix given in equation (6).

where

$$\boldsymbol{W}_t(\sigma) = \left(W_t(\phi^{(0)}, \sigma) \ W_t(\phi^{(1)}, \sigma) \ \ldots \ W_t(\phi^{(M-1)}, \sigma)\right) \tag{4}$$

Then (1) can be rewritten as

$$
\begin{aligned}
P_{\mathrm{b}} &= \lim_{t \to \infty} \frac{E[W_t(\sigma = 0)]}{tb} = \lim_{t \to \infty} \frac{\sum_{i=0}^{M-1} E[W_t(\phi^{(i)}, \sigma = 0)]}{tb} \\
&= \lim_{t \to \infty} \frac{E[\boldsymbol{W}_t(\sigma = 0)]\mathbf{1}_{1,M}^{\mathrm{T}}}{tb} = \lim_{t \to \infty} \frac{\boldsymbol{w}_t(\sigma = 0)\mathbf{1}_{1,M}^{\mathrm{T}}}{tb} \\
&= \lim_{t \to \infty} \frac{\boldsymbol{w}_t}{tb}\left(\mathbf{1}_{1,M} \ \mathbf{0}_{1,M} \ldots \mathbf{0}_{1,M}\right)^{\mathrm{T}} \tag{5}
\end{aligned}
$$

where $\mathbf{1}_{1,M}$ and $\mathbf{0}_{1,M}$ denote the all-one and the all-zero row vectors of length M, respectively, $\boldsymbol{w}_t$ represents the length $M|\Sigma|$ vector of the average information weights, while the length M vector of average information weights at the state σ is given by $\boldsymbol{w}_t(\sigma)$. Note that the mathematical expectations in (5) are computed over the sequences of channel noises and coin-flipping decisions.

To illustrate the introduced notations, we use the rate $R = 2/3$ memory $m = 1$, overall constraint length $\nu = 2$, minimal encoder with systematic generator matrix

$$G(D) = \begin{pmatrix} 1 & 0 & 1 + D \\ 0 & 1 & 1 + D \end{pmatrix} \tag{6}$$

It has a 2-state realization in observer canonical form as shown in Fig. 1.

Assuming that the normalized cumulative metric state is $\phi_t = 0$, we obtain the eight trellis sections given in Fig. 2. These trellis sections yield the normalized cumulative metric states $\{-1, 0, 1\}$. Using $\phi_t = -1$ and $\phi_t = 1$, we obtain 16 additional trellis sections and two additional normalized cumulative metric states $\{-2, 2\}$. From the metrics $\phi_t = -2$ and $\phi_t = 2$, we get another 16 trellis sections but those will not yield any new metrics. Thus, in total we have $M = 5$ normalized cumulative metric states $\phi_t \in \{-2, -1, 0, 1, 2\}$. Together with the eight different received triples, $\boldsymbol{r}_t = 000$, 001, 010, 100, 011, 101, 110, 111, they correspond to in total 40 different trellis sections. The bold branches in Fig. 2 correspond to the branches decided by the Viterbi decoder at time instant $t+1$. When we have more than one branch with maximum normalized cumulative metric entering the same state, we have a tie which we, in our analysis, resolve by fair coin-flipping.

Hence, the normalized cumulative metric Φ_t is a 5-state Markov chain with transition probability matrix $\Phi = (\phi_{jk})$, $1 \le j, k \le 5$.
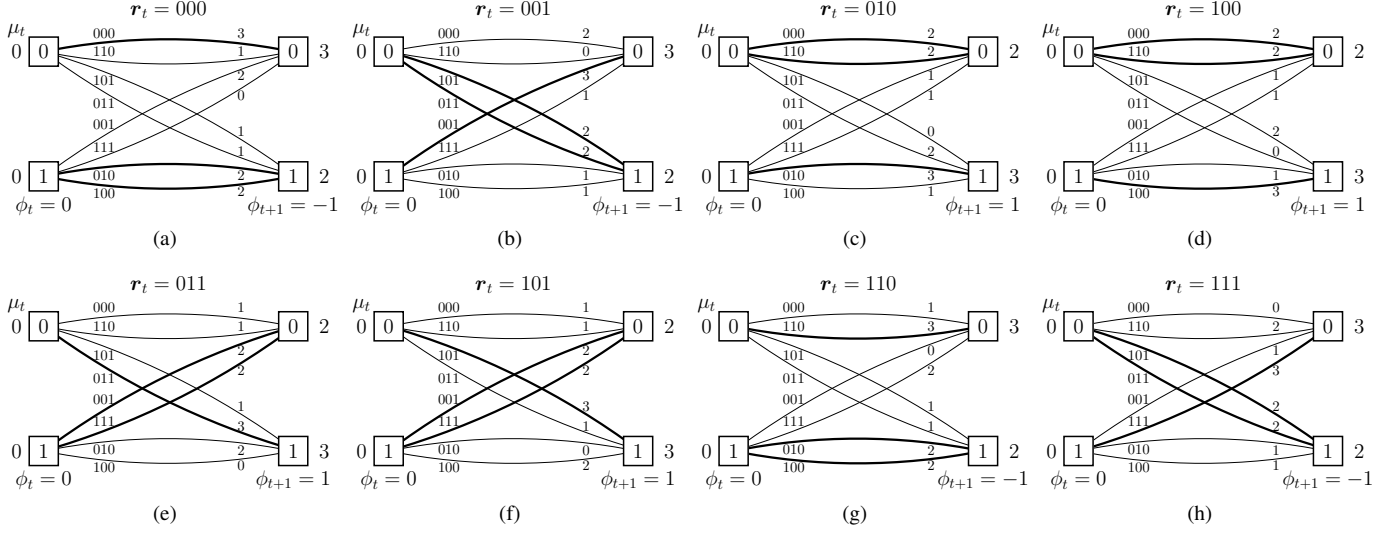
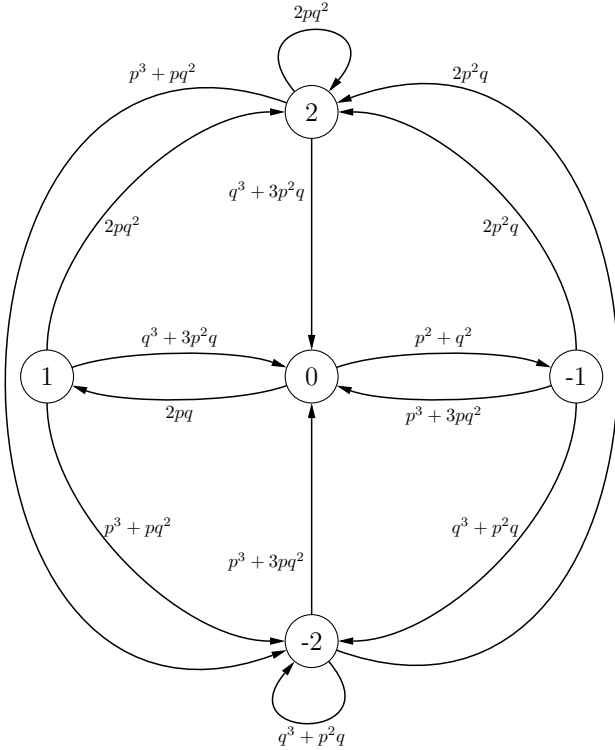Fig. 2: Eight (of a total of 40) trellis sections for the rate $R = 2/3$, 2-state encoder in Fig. 1.

Fig. 3: Illustration of the 5-state Markov chain formed by the sequences of normalized cumulative metric states ϕ_t.

From the four trellis sections, (a), (b), (g), and (h), in Fig. 2 we obtain

$$
\begin{aligned}
\phi_{0(-1)} &= \Pr\left(\boldsymbol{r}_t = 000\right) + \Pr\left(\boldsymbol{r}_t = 001\right) \\
&\quad + \Pr\left(\boldsymbol{r}_t = 110\right) + \Pr\left(\boldsymbol{r}_t = 111\right) \\
&= q^3 + pq^2 + p^2q + p^3 = p^2 + q^2
\end{aligned} \tag{7}
$$

while the four trellis sections, (c), (d), (e), and (f), yield

$$
\phi_{01} = pq^2 + pq^2 + p^2q + p^2q = 2pq \tag{8}
$$

where $q = 1 - p$.

Similarly, we can obtain the remaining transition probabilities from the 32 trellis sections not included in Fig. 2. Their transition probability matrix follows as

$$
\Phi = \begin{array}{c} \\ \mathbf{-2} \\ \mathbf{-1} \\ \mathbf{0} \\ \mathbf{1} \\ \mathbf{2} \\ \phi^{(j)} \end{array}
\begin{pmatrix}
\overset{\mathbf{-2}}{q^3 + p^2q} & \overset{\mathbf{-1}}{0} & \overset{\mathbf{0}}{p^3 + 3pq^2} & \overset{\mathbf{1}}{0} & \overset{\mathbf{2}}{2p^2q} \\
q^3 + p^2q & 0 & p^3 + 3pq^2 & 0 & 2p^2q \\
0 & p^2 + q^2 & 0 & 2pq & 0 \\
p^3 + pq^2 & 0 & q^3 + 3p^2q & 0 & 2p^2q \\
p^3 + pq^2 & 0 & q^3 + 3p^2q & 0 & 2p^2q
\end{pmatrix} \; \phi^{(k)} \tag{9}
$$

whose metric state Markov chain is shown in Fig. 3.

Let $\boldsymbol{p}_t$ denote the probabilities of the M different normalized cumulative metric values of Φ_t, that is, $\phi_t \in \{\phi^{(0)}, \phi^{(1)}, \ldots, \phi^{(M-1)}\}$. Their stationary distribution is denoted $\boldsymbol{p}_\infty = (p_\infty^{(0)} \; p_\infty^{(1)} \ldots p_\infty^{(M-1)})$ and is determined as the solution of, for example, the first $M - 1$ equations of

$$
\boldsymbol{p}_\infty \Phi = \boldsymbol{p}_\infty \tag{10}
$$

and

$$
\sum_{i=0}^{M-1} p_\infty^{(i)} = 1 \tag{11}
$$

For the 2-state convolutional encoder with generator matrix (6) we obtain

$$
\boldsymbol{p}_\infty^{\mathrm{T}} = \frac{1}{1 - p + 10p^2 - 20p^3 + 20p^4 - 8p^5}
$$
$$
\times \begin{pmatrix}
1 + 7p - 28p^2 + 66p^3 - 100p^4 + 96p^5 - 56p^6 + 16p^7 \\
- 3p + 16p^2 - 46p^3 + 80p^4 - 88p^5 + 56p^6 - 16p^7 \\
- 3p + 10p^2 - 20p^3 + 20p^4 - 8p^5 \\
- 6p^2 + 26p^3 - 60p^4 + 80p^5 - 56p^6 - 16p^7 \\
- 2p^2 - 6p^3 + 40p^4 - 72p^5 + 56p^6 - 16p^7
\end{pmatrix}
$$

In order to compute the exact bit error probability according to (5), it is necessary to determine $\boldsymbol{w}_t(\sigma = 0)$. In the next section we will derive a recurrent matrix equation for the average information weights and illustrate how to obtain its components using as an example the rate $R = 2/3$ memory $m = 1$ minimal encoder determined by (6).

III. Computing the Vector of Average Information Weights

The vector $\boldsymbol{w}_t$ describes the dynamics of the information weights when we proceed along the trellis and satisfies the recurrent equation

$$\begin{cases} \boldsymbol{w}_{t+1} = \boldsymbol{w}_t A + \boldsymbol{b}_t B \\ \boldsymbol{b}_{t+1} = \boldsymbol{b}_t \Pi \end{cases} \tag{12}$$

where A and B are $M|\Sigma| \times M|\Sigma|$ nonnegative matrices, Π is an $M|\Sigma| \times M|\Sigma|$ stochastic matrix, and $|\Sigma| = 2^m$. Both matrices consist of $|\Sigma| \times |\Sigma|$ submatrices A_{ij} and B_{ij} of size $M \times M$, respectively, where the former satisfy

$$\sum_{i=0}^{|\Sigma|-1} A_{ij} = \Phi - 1, \quad j = 0, 1, \ldots, |\Sigma| - 1 \tag{13}$$

since we consider only encoders for which every encoder state is reachable with probability 1.

The matrix A represents the linear part of the affine transformation of the information weights while the matrix B describes their increments. The submatrices A_{ij} and B_{ij} describe the updating of the average information weights if the transition from state i to state j exists; and are zero otherwise. Moreover, the vector $\boldsymbol{b}_t$ of length $M|\Sigma|$ is the concatenation of $|\Sigma|$ stochastic vectors $\boldsymbol{p}_t$, and hence the $M|\Sigma| \times M|\Sigma|$ matrix Π follows as

$$\Pi = \begin{pmatrix} \Phi & 0 & \ldots & 0 \\ 0 & \Phi & \ldots & 0 \\ \vdots & \vdots & \ddots & \vdots \\ 0 & 0 & \ldots & \Phi \end{pmatrix} \tag{14}$$

For simplicity, we choose the initial value of the vector of the information weights to be

$$\boldsymbol{w}_0 = \boldsymbol{0} \tag{15}$$

Continuing the previous example, we will illustrate how the 10×10 matrices A and B can be obtained directly from all 40 trellis sections. For example, the eight trellis sections in Fig. 2 determine all transitions from $\phi_t = 0$ to either $\phi_{t+1} = -1$ or $\phi_{t+1} = 1$.

To be more specific, consider all transitions from $\sigma_t = 0$ and $\phi_t = 0$ to $\sigma_{t+1} = 0$ and $\phi_{t+1} = -1$, as shown in Fig. 2(a), (b), (g), and (h). Only Fig. 2(a) and (g) have transitions decided by the Viterbi algorithm, which are $\boldsymbol{v}_t = 000$ in Fig. 2(a) and $\boldsymbol{v}_t = 110$ in Fig. 2(g), and thus the entry $\sigma_t = 0$, $\phi_t = 0$, $\sigma_{t+1} = 0$, $\phi_{t+1} = -1$ in matrix A follows as

$$\Pr(\boldsymbol{r}_t = 000) + \Pr(\boldsymbol{r}_t = 110) = q^3 + p^2 q$$

and in matrix B as

$$\beta(000)\Pr(\boldsymbol{r}_t = 000) + \beta(110)\Pr(\boldsymbol{r}_t = 110) \\ = 0 + 2p^2 q = 2p^2 q$$

where $\beta(\boldsymbol{v}_t)$ denotes the number of information 1s corresponding to $\boldsymbol{v}_t$. Since we use coin-flipping to resolve ties,

we obtain that the entry $\sigma_t = 0$, $\phi_t = 0$, $\sigma_{t+1} = 0$, $\phi_{t+1} = 1$ (Fig. 2(c) and (d)) in matrix A is

$$\frac{1}{2}\Pr(\boldsymbol{r}_t = 010) + \frac{1}{2}\Pr(\boldsymbol{r}_t = 010)$$
$$+ \frac{1}{2}\Pr(\boldsymbol{r}_t = 100) + \frac{1}{2}\Pr(\boldsymbol{r}_t = 100)$$
$$= \frac{1}{2}pq^2 + \frac{1}{2}pq^2 + \frac{1}{2}pq^2 + \frac{1}{2}pq^2 = 2pq^2$$

and in matrix B

$$\frac{1}{2}\beta(000)\Pr(\boldsymbol{r}_t = 010) + \frac{1}{2}\beta(110)\Pr(\boldsymbol{r}_t = 010)$$
$$+ \frac{1}{2}\beta(000)\Pr(\boldsymbol{r}_t = 100) + \frac{1}{2}\beta(110)\Pr(\boldsymbol{r}_t = 100)$$
$$= \frac{1}{2} \cdot 0 + \frac{1}{2} \cdot 2pq^2 + \frac{1}{2} \cdot 0 + \frac{1}{2} \cdot 2pq^2 = 2pq^2$$

Similarly the entry $\sigma_t = 1$, $\phi_t = 0$, $\sigma_{t+1} = 0$, $\phi_{t+1} = -1$ (Fig. 2(b) and (h)) in matrix A is

$$pq^2 + p^3$$

and in matrix B

$$0 + 2p^3 = 2p^3$$

Finally, the entry $\sigma_t = 1$, $\phi_t = 0$, $\sigma_{t+1} = 0$, $\phi_{t+1} = 1$ (Fig. 2(e) and (f)) in matrix A is given by

$$\frac{1}{2}p^2 q + \frac{1}{2}p^2 q + \frac{1}{2}p^2 q + \frac{1}{2}p^2 q = 2p^2 q$$

and in matrix B by

$$\frac{1}{2} \cdot 0 + \frac{1}{2} \cdot 2p^2 q + \frac{1}{2} \cdot 0 + \frac{1}{2} \cdot 2p^2 q = 2p^2 q$$

The trellis sections in Fig. 2 determine also the entries for the transitions $\sigma_t = 0$, $\phi_t = 0$, $\sigma_{t+1} = 1$, $\phi_{t+1} = -1$ and $\sigma_t = 0$, $\phi_t = 0$, $\sigma_{t+1} = 1$, $\phi_{t+1} = 1$ as well as the transitions $\sigma_t = 1$, $\phi_t = 0$, $\sigma_{t+1} = 1$, $\phi_{t+1} = -1$ and $\sigma_t = 1$, $\phi_t = 0$, $\sigma_{t+1} = 1$, $\phi_{t+1} = 1$.

The remaining transitions with $\phi_t = 0$ are never decided by the Viterbi algorithm, and hence the corresponding entries are zero. The eight trellis sections in Fig. 2 yield 20 entries in the matrices A and B, while the 32 trellis sections not shown in Fig. 2 yield the remaining 80 entries. For the convolutional encoder shown in Fig. 1 we obtain

$$A = \begin{pmatrix} A_{00} & A_{01} \\ A_{10} & A_{11} \end{pmatrix} \tag{16}$$

where

$$A_{00} = \begin{array}{c} \\ -2 \\ -1 \\ 0 \\ 1 \\ 2 \end{array} \begin{pmatrix} q^3+p^2q & 0 & p^3+3pq^2 & 0 & 2p^2q \\ q^3+p^2q & 0 & \frac{1}{2}p^3+\frac{5}{2}pq^2 & 0 & p^2q \\ 0 & q^3+p^2q & 0 & 2pq^2 & 0 \\ 0 & 0 & \frac{1}{2}q^3+\frac{1}{2}p^2q & 0 & pq^2 \\ 0 & 0 & 0 & 0 & 0 \end{pmatrix} \tag{17}$$

with column labels $-2, -1, 0, 1, 2$.

$$A_{01} = \begin{array}{c} \\ -2 \\ -1 \\ 0 \\ 1 \\ 2 \end{array} \begin{pmatrix} p^2q+q^3 & 0 & p^3+3pq^2 & 0 & 2p^2q \\ \frac{1}{2}p^3+\frac{1}{2}pq^2 & 0 & p^2q & 0 & 0 \\ 0 & p^3+pq^2 & 0 & 2p^2q & 0 \\ \frac{1}{2}q^3+\frac{1}{2}p^2q & 0 & p^3+2pq^2 & 0 & 2p^2q \\ 0 & 0 & 0 & 0 & 0 \end{pmatrix} \tag{18}$$

with column labels $-2, -1, 0, 1, 2$.

$$A_{10} = \begin{array}{c} \\ \text{-2} \\ \text{-1} \\ \mathbf{0} \\ \mathbf{1} \\ \mathbf{2} \end{array} \begin{array}{ccccc} \text{-2} & \text{-1} & \mathbf{0} & \mathbf{1} & \mathbf{2} \\ 0 & 0 & 0 & 0 & 0 \\ 0 & 0 & \frac{1}{2}p^3+\frac{1}{2}pq^2 & 0 & p^2q \\ 0 & p^3+pq^2 & 0 & 2p^2q & 0 \\ p^3+pq^2 & 0 & \frac{1}{2}q^3+\frac{5}{2}p^2q & 0 & pq^2 \\ p^3+pq^2 & 0 & 3p^2q+q^3 & 0 & 2pq^2 \end{array} \qquad (19)$$

$$A_{11} = \begin{array}{c} \\ \text{-2} \\ \text{-1} \\ \mathbf{0} \\ \mathbf{1} \\ \mathbf{2} \end{array} \begin{array}{ccccc} \text{-2} & \text{-1} & \mathbf{0} & \mathbf{1} & \mathbf{2} \\ 0 & 0 & 0 & 0 & 0 \\ \frac{1}{2}p^2q+\frac{1}{2}q^3 & 0 & pq^2 & 0 & 0 \\ 0 & p^2q+q^3 & 0 & 2pq^2 & 0 \\ \frac{1}{2}pq^2+\frac{1}{2}p^3 & 0 & 2p^2q+q^3 & 0 & 2pq^2 \\ p^3+pq^2 & 0 & 3p^2q+q^3 & 0 & 2pq^2 \end{array} \qquad (20)$$

and

$$B = \begin{pmatrix} B_{00} & B_{01} \\ B_{10} & B_{11} \end{pmatrix} \qquad (21)$$

where

$$B_{00} = \begin{array}{c} \\ \text{-2} \\ \text{-1} \\ \mathbf{0} \\ \mathbf{1} \\ \mathbf{2} \end{array} \begin{array}{ccccc} \text{-2} & \text{-1} & \mathbf{0} & \mathbf{1} & \mathbf{2} \\ 2p^2q & 0 & p^3+2pq^2 & 0 & 2p^2q \\ 0 & 0 & p^2q & 0 & pq^2 \\ 0 & 2p^2q & 0 & 2pq^2 & 0 \\ 2p^2q & 0 & p^3+2pq^2 & 0 & p^2q \\ 0 & 0 & 0 & 0 & 0 \end{array} \qquad (22)$$

$$B_{01} = \begin{array}{c} \\ \text{-2} \\ \text{-1} \\ \mathbf{0} \\ \mathbf{1} \\ \mathbf{2} \end{array} \begin{array}{ccccc} \text{-2} & \text{-1} & \mathbf{0} & \mathbf{1} & \mathbf{2} \\ p^2q+q^3 & 0 & p^3+3pq^2 & 0 & 2p^2q \\ \frac{1}{2}p^3+\frac{1}{2}pq^2 & 0 & p^2q & 0 & 0 \\ 0 & p^3+pq^2 & 0 & 2p^2q & 0 \\ \frac{1}{2}q^3+\frac{1}{2}p^2q & 0 & p^3+2pq^2 & 0 & 2p^2q \\ 0 & 0 & 0 & 0 & 0 \end{array} \qquad (23)$$

$$B_{10} = \begin{array}{c} \\ \text{-2} \\ \text{-1} \\ \mathbf{0} \\ \mathbf{1} \\ \mathbf{2} \end{array} \begin{array}{ccccc} \text{-2} & \text{-1} & \mathbf{0} & \mathbf{1} & \mathbf{2} \\ 0 & 0 & 0 & 0 & 0 \\ 0 & 0 & p^3 & 0 & p^2q \\ 0 & 2p^3 & 0 & 2p^2q & 0 \\ 2p^3 & 0 & 3p^2q & 0 & pq^2 \\ 2p^3 & 0 & 4p^2q & 0 & 2pq^2 \end{array} \qquad (24)$$

$$B_{11} = \begin{array}{c} \\ \text{-2} \\ \text{-1} \\ \mathbf{0} \\ \mathbf{1} \\ \mathbf{2} \end{array} \begin{array}{ccccc} \text{-2} & \text{-1} & \mathbf{0} & \mathbf{1} & \mathbf{2} \\ 0 & 0 & 0 & 0 & 0 \\ \frac{1}{2}p^2q+\frac{1}{2}q^3 & 0 & pq^2 & 0 & 0 \\ 0 & p^2q+q^3 & 0 & 2pq^2 & 0 \\ \frac{1}{2}pq^2+\frac{1}{2}p^3 & 0 & 2p^2q+q^3 & 0 & 2pq^2 \\ p^3+pq^2 & 0 & 3p^2q+q^3 & 0 & 2pq^2 \end{array} \qquad (25)$$

IV. SOLVING THE RECURRENT EQUATION

Consider the second equation in (12). It follows from (5) that we are only interested in the asymptotic values, and hence letting t tend to infinity yields

$$\boldsymbol{b}_\infty = \boldsymbol{b}_\infty \Pi \qquad (26)$$

where $\boldsymbol{b}_\infty$ can be chosen as

$$\boldsymbol{b}_\infty = (\boldsymbol{p}_\infty \, \boldsymbol{p}_\infty \ldots \boldsymbol{p}_\infty) \qquad (27)$$

To obtain the last equality, we took into account that Π is a block-diagonal matrix whose diagonal elements are given by the transition probability matrix Φ which satisfies (10). Based on these observations, (12) can be simplified to

$$\boldsymbol{w}_{t+1} = \boldsymbol{w}_t A + \boldsymbol{b}_\infty B \qquad (28)$$

By iterating the recurrent equation (28) and using the initial value (15), the vector of the information weights at time instant $t+1$ is given by

$$\boldsymbol{w}_{t+1} = \boldsymbol{b}_\infty B A^t + \boldsymbol{b}_\infty B A^{t-1} + \cdots + \boldsymbol{b}_\infty B \qquad (29)$$

Taking its limit, it follows that

$$\lim_{t\to\infty} \frac{\boldsymbol{w}_t}{tb} = \lim_{t\to\infty} \frac{\boldsymbol{w}_{t+1}}{tb} = \lim_{t\to\infty} \frac{1}{tb} \sum_{j=0}^{t} \boldsymbol{b}_\infty B A^{t-j}$$
$$= \boldsymbol{b}_\infty B A^\infty / b \qquad (30)$$

where A^∞ denotes the limit of the sequence A^t when t tends to infinity and we used the fact that, if a sequence converges to a finite limit, then it is Cesàro-summable to the same limit.

From (13) it follows that

$$\boldsymbol{e}_\mathrm{L} = (\boldsymbol{p}_\infty \, \boldsymbol{p}_\infty \ldots \boldsymbol{p}_\infty) \qquad (31)$$

satisfies

$$\boldsymbol{e}_\mathrm{L} A = \boldsymbol{e}_\mathrm{L} \qquad (32)$$

and hence $\boldsymbol{e}_\mathrm{L}$ is a left eigenvector with eigenvalue $\lambda = 1$. Due to the nonnegativity of A, $\lambda = 1$ is a maximal eigenvalue of A (Corollary 8.1.30 [7]). Let $\boldsymbol{e}_\mathrm{R}$ denote the right eigenvector corresponding to the eigenvalue $\lambda = 1$ normalized such that $\boldsymbol{e}_\mathrm{L} \boldsymbol{e}_\mathrm{R} = 1$. If we remove the allzero rows and corresponding columns from the matrix A we obtain an irreducible matrix which has a unique maximal eigenvalue $\lambda = 1$ (Lemma 8.4.3 [7]). Hence, it follows (Lemma 8.2.7, statement (i) [7]) that

$$A^\infty = \boldsymbol{e}_\mathrm{R} \boldsymbol{e}_\mathrm{L} \qquad (33)$$

Combining (30), (31), and (33) yields

$$\lim_{t\to\infty} \frac{\boldsymbol{w}_t}{tb} = \boldsymbol{b}_\infty B \boldsymbol{e}_\mathrm{R} (\boldsymbol{p}_\infty \, \boldsymbol{p}_\infty \ldots \boldsymbol{p}_\infty)/b \qquad (34)$$

Following (5), by summing up the first M components of the vector $(\boldsymbol{p}_\infty \, \boldsymbol{p}_\infty \ldots \boldsymbol{p}_\infty)$ on the right side of (34), we obtain the closed form expression for the exact bit error probability as

$$P_\mathrm{b} = \boldsymbol{b}_\infty B \boldsymbol{e}_\mathrm{R} / b \qquad (35)$$
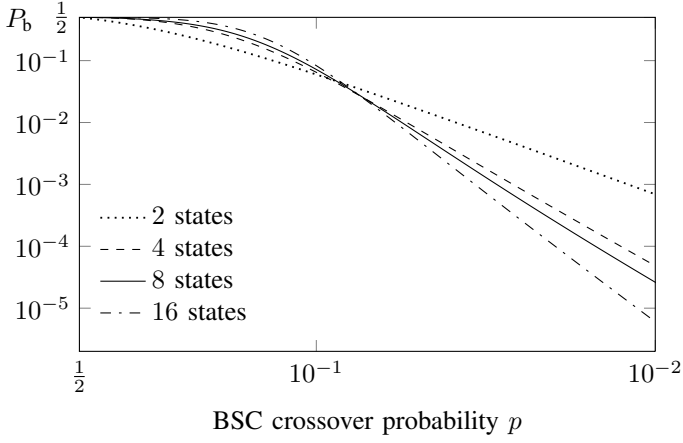
Fig. 4: Exact bit error probability for the rate $R = 1/2$ minimal encoders of memory $m = 1$ (2-state) $G(D) = (1 \quad 1 + D)$, memory $m = 2$ (4-state) $G(D) = (1 + D^2 \quad 1 + D + D^2)$, memory $m = 3$ (8-state) $G(D) = (1 + D^2 + D^3 \quad 1 + D + D^2 + D^3)$, and memory $m = 4$ (16-state) $G(D) = (1 + D + D^4 \quad 1 + D + D^2 + D^3 + D^4)$.

To summarize, the exact bit error probability P_b for Viterbi decoding of a rate $R = b/c$ minimal convolutional encoder, when communicating over the BSC, is calculated as follows:

- Construct the set of metric states and find the stationary probability distribution $\boldsymbol{p}_\infty$.
- Determine the matrices A and B as in Section II and compute the right eigenvector $\boldsymbol{e}_R$ normalized according to $(\boldsymbol{p}_\infty \ \boldsymbol{p}_\infty \dots \boldsymbol{p}_\infty)\boldsymbol{e}_R = 1$.
- Calculate the exact bit error probability P_b using (35).

For the encoder shown in Fig. 1 we obtain

$$
\begin{aligned}
P_b = &\big(4p - 2p^2 + 67p^3 - 320p^4 + 818p^5 - 936p^6 - 884p^7 \\
&+ 5592p^8 - 11232p^9 + 13680p^{10} - 11008p^{11} \\
&+ 5760p^{12} - 1792p^{13} + 256p^{14}\big) / \big(2 - 5p + 41p^2 \\
&- 128p^3 + 360p^4 - 892p^5 + 1600p^6 - 1904p^7 \\
&+ 1440p^8 - 640p^9 + 128p^{10}\big) \\
= &\, 2p + 4p^2 + \frac{5}{2}p^3 - \frac{431}{4}p^4 - \frac{125}{8}p^5 + \frac{32541}{16}p^6 \\
&- \frac{70373}{32}p^7 - \frac{1675587}{64}p^8 + \frac{7590667}{128}p^9 \\
&+ \frac{67672493}{256}p^{10} - \cdots
\end{aligned}
\tag{36}
$$

If we instead realize the *minimal* generator matrix (6) in controller canonical form, we obtain a *nonminimal* (4-state) encoder with $M = 12$ normalized cumulative metric state; *cf.*, the Remark after (1). Its exact bit error probability is slightly worse than that of its minimal realization in observer canonical form.

V. SOME EXAMPLES

First we consider some rate $R = 1/2$, memory $m = 1, 2, 3$, and 4 convolutional encoders; that is, encoders with $2, 4, 8$, and 16 states, realized in controller canonical form. In Fig. 4 we plot the exact bit error probability for those four convolutional encoders.

Example 1: If we draw all 20 trellis sections for the rate $R = 1/2$, memory $m = 1$ (2-state) convolutional encoder with generator matrix $G(D) = (1 \quad 1 + D)$ realized in controller canonical form, we obtain the normalized cumulative metric states $\{-2, -1, 0, 1, 2\}$. Its metric state Markov chain yields the stationary probability distribution

$$
\boldsymbol{p}_\infty^T = \frac{1}{1 + 3p^2 - 2p^3}
\begin{pmatrix}
1 - 4p + 8p^2 - 7p^3 + 2p^4 \\
2p - 5p^2 + 5p^3 - 2p^4 \\
2p - 3p^2 + 3p^3 \\
2p^2 - 3p^3 + 2p^4 \\
p^2 + p^3 - 2p^4
\end{pmatrix}
\tag{37}
$$

Based on these 20 trellis sections, the 10×10 matrices A and B are constructed as

$$
A = \begin{pmatrix} A_{00} & A_{01} \\ A_{10} & A_{11} \end{pmatrix}
\tag{38}
$$

and

$$
B = \begin{pmatrix} \mathbf{0}_{5,5} & A_{01} \\ \mathbf{0}_{5,5} & A_{11} \end{pmatrix}
\tag{39}
$$

where $\mathbf{0}_{5,5}$ denotes the 5×5 all-zero matrix. The normalized right eigenvector of A is

$$
\boldsymbol{e}_R =
\begin{pmatrix}
0 \\
0 \\
0 \\
0 \\
0 \\
0 \\
\dfrac{pq}{2} \\
\dfrac{4pq}{2 - p + 4p^2 - 4p^3} \\
\dfrac{(2 + 7p - 12p^2 + 13p^3 - 12p^4 + 4p^5)}{2(2 - p + 4p^2 - 4p^3)} \\
1
\end{pmatrix}
\tag{40}
$$

Finally, inserting (37), (39), and (40) into (35) yields the following expression for the exact bit error probability

$$
\begin{aligned}
P_b &= \frac{14p^2 - 23p^3 + 16p^4 + 2p^5 - 16p^6 + 8p^7}{(1 + 3p^2 - 2p^3)(2 - p + 4p^2 - 4p^3)} \\
&= 7p^2 - 8p^3 - 31p^4 + 64p^5 + 86p^6 - \frac{635}{2}p^7 \\
&\quad - \frac{511}{4}p^8 + \frac{10165}{8}p^9 - \frac{4963}{16}p^{10} - \cdots
\end{aligned}
\tag{41}
$$

which coincides with the exact bit error probability formula given in [4].

Example 2: For the rate $R = 1/2$, memory $m = 2$ (4-state) convolutional encoder with generator matrix $G(D) = (1 + D^2 \quad 1 + D + D^2)$ realized in controller canonical form, we obtain, for example, the four trellis sections for $\phi_t = (0\,0\,0)$ shown in Fig. 5. The corresponding metric states at times $t+1$ are $\phi_{t+1} = (-1\,0\,-1)$ and $\phi_{t+1} = (1\,0\,1)$.

Completing the set of trellis sections yields in total $M = 31$ different normalized cumulative metric states, and hence the 124×124 matrices A and B have the following block structure
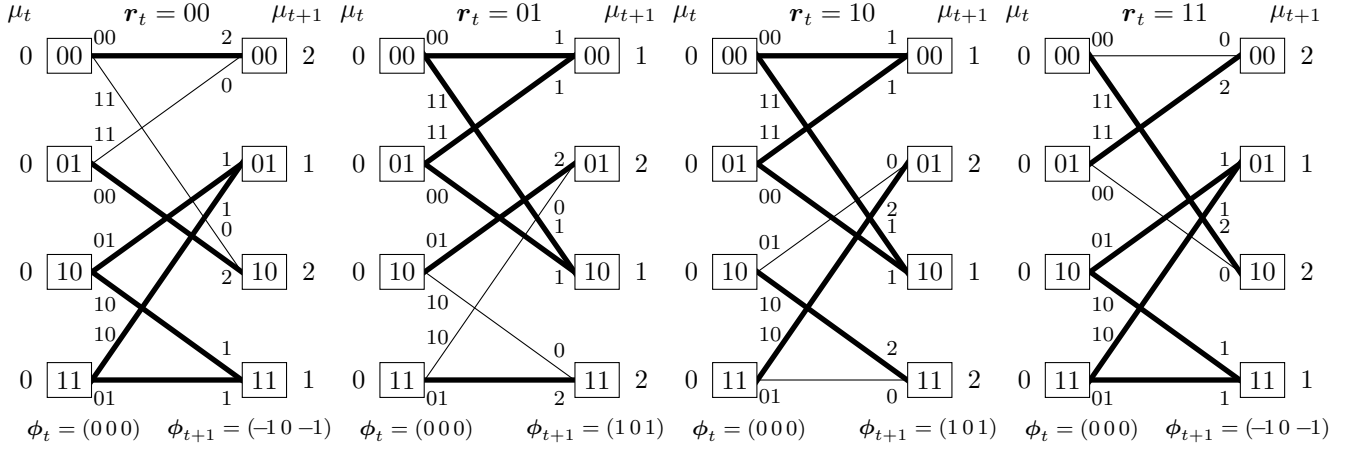
Fig. 5: Four different trellis sections of the in total 124 for the $G(D) = (1 + D^2 \quad 1 + D + D^2)$ generator matrix.

$$A = \begin{pmatrix} A_{00} & \mathbf{0}_{31,31} & A_{02} & \mathbf{0}_{31,31} \\ A_{10} & \mathbf{0}_{31,31} & A_{12} & \mathbf{0}_{31,31} \\ \mathbf{0}_{31,31} & A_{21} & \mathbf{0}_{31,31} & A_{23} \\ \mathbf{0}_{31,31} & A_{31} & \mathbf{0}_{31,31} & A_{33} \end{pmatrix} \quad (42)$$

and

$$B = \begin{pmatrix} \mathbf{0}_{31,31} & \mathbf{0}_{31,31} & A_{02} & \mathbf{0}_{31,31} \\ \mathbf{0}_{31,31} & \mathbf{0}_{31,31} & A_{12} & \mathbf{0}_{31,31} \\ \mathbf{0}_{31,31} & \mathbf{0}_{31,31} & \mathbf{0}_{31,31} & A_{23} \\ \mathbf{0}_{31,31} & \mathbf{0}_{31,31} & \mathbf{0}_{31,31} & A_{33} \end{pmatrix} \quad (43)$$

Following the method for calculating the exact bit error probability described in Section IV we obtain

$$P_{\mathsf{b}} = 44p^3 + \frac{3519}{8}p^4 - \frac{14351}{32}p^5 - \frac{1267079}{64}p^6 \\ - \frac{31646405}{512}p^7 + \frac{978265739}{2048}p^8 \\ + \frac{3931764263}{1024}p^9 - \frac{48978857681}{32768}p^{10} - \cdots \quad (44)$$

which coincides with the previously obtained result by Lentmaier et al. [6].

Example 3: For the rate $R = 1/2$, memory $m = 3$ (8-state) convolutional encoder with generator matrix $G(D) = (1 + D^2 + D^3 \quad 1 + D + D^2 + D^3)$ realized in controller canonical form we have $M = 433$ normalized cumulative metric states and the A and B matrices are of size $433 \cdot 2^3 \times 433 \cdot 2^3$.

Since the complexity of the symbolic derivations increases greatly, we can only obtain a numerical solution of (35), as shown in Fig. 4.

Example 4: For the rate $R = 1/2$, memory $m = 4$ (16-state) convolutional encoder with generator matrix $G(D) = (1 + D^2 + D^3 + D^4 \quad 1 + D + D^4)$ realized in controller canonical form, we have as many as $M = 188687$ normalized cumulative metric states. Thus, the matrices A and B are of size $188687 \cdot 2^4 \times 188687 \cdot 2^4$. The corresponding numerical solution of (35) is plotted in Fig. 4.

The obvious next step is to try a rate $R = 1/2$, memory $m = 5$ (32-state) convolutional encoder. We tried the generator matrix $G(D) = (1 + D + D^2 + D^3 + D^4 + D^5 \quad 1 + D^3 + D^5)$ realized in controller canonical form but were only able to show that the number of cumulative normalized metric states M exceeds 4130000.

Example 5: Consider the generator matrix $G_1(D) = (1 + D^2 \quad 1 + D + D^2)$ and its equivalent systematic generator matrices $G_2(D) = (1 \quad (1+D^2)/(1+D+D^2))$ and $G_3(D) = (1 \quad (1 + D + D^2)/(1 + D^2))$. When realized in controller canonical form, all three realizations have $M = 31$ normalized cumulative metric states. The exact bit error probability for $G_1(D)$ is given by (44). For $G_2(D)$ and $G_3(D)$ we obtain

$$P_{\mathsf{b}} = \frac{163}{2}p^3 + \frac{365}{2}p^4 - \frac{24045}{8}p^5 - \frac{1557571}{128}p^6 \\ + \frac{23008183}{512}p^7 + \frac{1191386637}{2048}p^8 \\ + \frac{4249634709}{8192}p^9 + \frac{132555764497}{8192}p^{10} - \cdots \quad (45)$$

and

$$P_{\mathsf{b}} = \frac{141}{2}p^3 + \frac{1739}{8}p^4 - \frac{71899}{32}p^5 - \frac{1717003}{128}p^6 \\ + \frac{2635041}{128}p^7 + \frac{540374847}{1024}p^8 \\ + \frac{9896230051}{8192}p^9 - \frac{402578056909}{32768}p^{10} - \cdots \quad (46)$$

respectively. The corresponding numerical results are illustrated in Fig. 6.
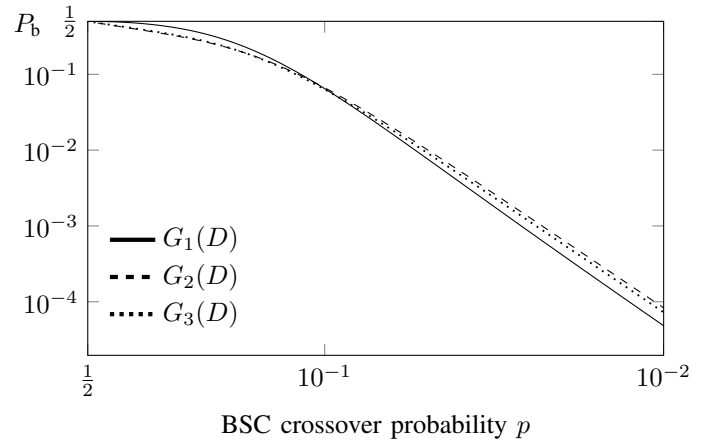

Fig. 6: Exact bit error probability for the rate $R = 1/2$ memory $m = 2$ minimal encoders with $G_1(D) = (1 + D^2 \quad 1 + D + D^2)$, $G_2(D) = (1 \quad (1+D^2)/(1+D+D^2))$, and $G_3(D) = (1 \quad (1 + D + D^2)/(1 + D^2))$.
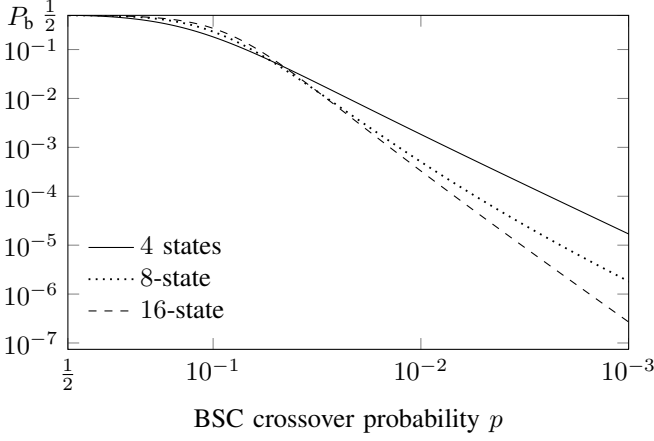
Fig. 7: Exact bit error probability for the rate $R = 2/3$, overall constraint length $\nu = 2, 3$, and 4 (4-state, 8-state, and 16-state, respectively) minimal encoders whose generator matrices are given in Table I.

TABLE I: Rate $R = 2/3$ generator matrices

$G(D)$	#states	d_{free}	M
$\begin{pmatrix} D & 1+D & 1+D \\ 1 & D & 1+D \end{pmatrix}$	4	3	19
$\begin{pmatrix} 1+D & D & 1 \\ D^2 & 1 & 1+D+D^2 \end{pmatrix}$	8	4	347
$\begin{pmatrix} D+D^2 & 1 & 1+D^2 \\ 1 & D+D^2 & 1+D+D^2 \end{pmatrix}$	16	5	15867

Example 6: The exact bit error probabilities for the rate $R = 2/3$ 4-state, 8-state, and 16-state generator matrices, given in Table I and realized in controller canonical form, are plotted in Fig. 7.

As an example, the 4-state encoder has the exact bit error probability

$$P_{\text{b}} = \frac{67}{2}p^2 + \frac{17761}{48}p^3 - \frac{2147069}{648}p^4 - \frac{1055513863}{46656}p^5$$
$$+ \frac{123829521991}{559872}p^6 + \frac{67343848419229}{60466176}p^7$$
$$- \frac{27081094434882419}{2176782336}p^8 - \frac{477727138796620247}{8707129344}p^9$$
$$+ \frac{19448293197633324 73469}{2821109907456}p^{10} + \cdots \quad (47)$$

If we replace the BSC with the quantized additive white Gaussian noise (AWGN) channel, the calculation of the exact bit error probability follows the same method as described in Section IV, but the computational complexity increases dramatically as illustrated by the following example.

Example 7: Consider the generator matrix $G(D) = (1 + D^2 \quad 1 + D + D^2)$ used to communicate over a quantized AWGN channel. We use different quantization methods, namely, uniform quantization [8], [9] and Massey quantization [10], [11]; see Fig. 9.
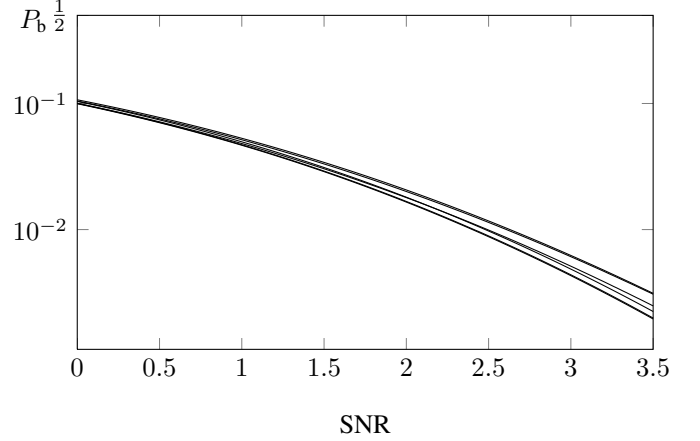

Fig. 8: Exact bit error probability for the rate $R = 1/2$, memory $m = 2$ (4-state) encoder with $G(D) = (1 + D^2 \quad 1 + D + D^2)$ used to communicate over an AWGN channel with different quantization levels.
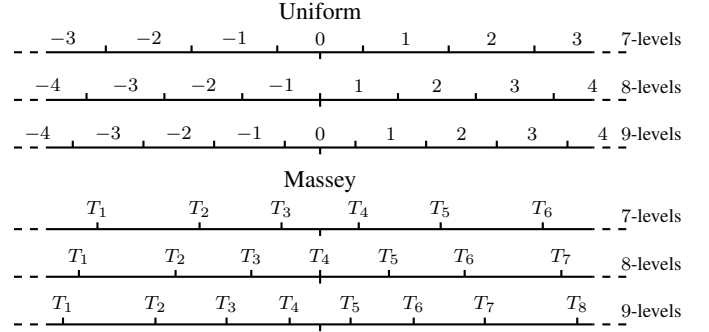

Fig. 9: Examples of uniform and Massey quantizations for an AWGN channel with SNR = 0dB.

The uniform intervals were determined by optimizing the cut-off rate R_0. The Massey quantization thresholds T_i between intervals were also determined by optimizing R_0, but allowing for nonuniform intervals. The realization in controller canonical form yields that, for all signal to noise ratios (SNRs), E_{b}/N_0, and uniform quantization with 7, 8, and 9 levels, the number of the normalized cumulative metric states is $M = 1013$, $M = 2143$, and $M = 2281$, respectively. However, for the Massey quantization the number of normalized cumulative metric states varies with both the number of levels and the SNR. Moreover, these numbers are much higher. For example, considering the interval between 0 dB and 3.5 dB with 8 quantization levels, we have $M = 16639$ for $E_{\text{b}}/N_0 \leq 2.43$ dB, while for $E_{\text{b}}/N_0 > 2.43$ dB we obtain $M = 17019$. The exact bit error probability for this 4-state encoder is plotted for all different quantizations in Fig. 8, ordered from worst (top) to best (bottom) as

   (i) Uniform 8 levels
  (ii) Uniform 7 levels
 (iii) Massey 7 levels
 (iv) Uniform 9 levels
  (v) Massey 8 levels
 (vi) Massey 9 levels

All differences are very small, and hence it is hard to distinguish all the curves. It is interesting to notice that using 7 instead of 8 uniform quantization levels yields a better bit error probability. However, this is not surprising since the presence of a quantization bin around zero typically improves the quantization performance. Moreover, the number of cumulative normalized metric states for 7 quantization levels is only about one half of that for 8 quantization levels. Notice that such a subtle comparison of channel output quantizers has only become possible due to the closed form expression for the exact bit error probability.

VI. CONCLUSION

We have derived a closed form expression for the exact bit error probability for Viterbi decoding of convolutional codes using a recurrent matrix equation. In particular, the described method is feasible to evaluate the performance of encoders with as many as 16 states when communicating over the BSC. By applying our new approach to a 4-state encoder used to communicate over the quantized AWGN channel, the expression for the exact error probability for Viterbi decoding is also derived. In particular, it is shown that the proposed technique can be used to select the optimal encoder implementation as well as the optimal channel output quantizer based on comparing their corresponding exact bit decoding error probability.

REFERENCES

[1] A. J. Viterbi, "Convolutional codes and their performance in communication systems," *IEEE Trans. Inf. Theory*, vol. IT-19, no. 5, pp. 751–772, Oct. 1971.
[2] L. Van de Meeberg, "A tightened upper bound on the error probability of binary convolutional codes with viterbi decoding," *IEEE Trans. Inf. Theory*, vol. IT-20, no. 3, pp. 389–391, Oct. 1974.
[3] T. N. Morrissey, Jr., "Analysis of decoders for convolutional codes by stochastic sequential machine methods," *IEEE Trans. Inf. Theory*, vol. IT-16, no. 4, pp. 460–469, Jul. 1970.
[4] M. R. Best, M. V. Burnashev, Y. Levy, A. Rabinovich, P. C. Fishburn, A. R. Calderbank, and D. J. Costello, Jr., "On a technique to calculate the exact performance of a convolutional code," *IEEE Trans. Inf. Theory*, vol. 41, no. 2, pp. 441–447, Mar. 1995.
[5] M. V. Burnashev and D. L. Cohn, "Symbol error probability for convolutional codes," *Problems on Information Transmission*, vol. 26, no. 4, pp. 289–298, 1990.
[6] M. Lentmaier, D. V. Truhachev, and K. S. Zigangirov, "Analytic expressions for the bit error probabilities of rate-1/2 memory 2 convolutional encoders," *IEEE Trans. Inf. Theory*, vol. 50, no. 6, pp. 1303–1311, Jun. 2004.
[7] R. A. Horn and C. R. Johnson, *Matrix Analysis*. Cambridge University Press, Feb. 1990.
[8] J. A. Heller and I. M. Jacobs, "Viterbi decoding for satellite and space communication," *IEEE Trans. Commun.*, vol. COM-19, no. 5, pp. 835–848, Oct. 1971.
[9] I. M. Onyszchuk, K.-M. Cheung, and O. Collins, "Quantization loss in convolutional decoding," *IEEE Trans. Commun.*, vol. 41, no. 2, pp. 261–265, Feb. 1993.
[10] J. L. Massey, "Coding and modulation in digital communications," in *Proc. Int. Zurich Seminar on Digital Communications*, Zurich, Mar. 12–25, 1974.
[11] R. Johannesson and K. S. Zigangirov, *Fundamentals of Convolutional Coding*. Piscataway, NJ: IEEE Press, 1999.

Irina E. Bocharova was born in Leningrad, U.S.S.R., on July 31, 1955. She received the Diploma in Electrical Engineering in 1978 from the Leningrad Electro-Technical Institute and the Ph.D. degree in technical sciences in 1986 from the Leningrad Institute of Aerospace Instrumentation.

During 1986-2007, she has been a Senior Researcher, an Assistant Professor, and then Associate Professor at the Leningrad Institute of Aerospace Instrumentation (now State University of Aerospace Instrumentation, St.-Petersburg, Russia). Since 2007 she has been an Associate Professor at the State University of Information Technologies, Mechanics and Optics. Her research interests include convolutional codes, communication systems, source coding and its applications to speech, audio and image coding. She has published more than 50 papers in journals and proceedings of international conferences, and seven U.S. patents in speech, audio and video coding. She has authored the textbook *Compression for Multimedia* (Cambridge University Press, 2010).

Professor Bocharova was awarded the Lise Meitner Visiting Chair in engineering at Lund University, Lund, Sweden (January–June 2005 and 2011).

Florian Hug (S'08) was born in Memmingen, Germany, on May 21, 1983. He received the Dipl.-Ing. degree from the Faculty of Electrical Engineering, University of Ulm, Ulm, Germany, in 2008. Since then, he has been with the Department of Electrical and Information Technology, Lund University, Lund, Sweden, where he is working towards the Ph.D. degree in information theory. His research interests covers the field of information and coding theory. Currently, he is focusing on codes over graphs.

Rolf Johannesson (M'72, F'98, LF'12) was born in Hässleholm, Sweden, on July 3, 1946. He received the M.S. and Ph.D. degrees in 1970 and 1975, respectively, both from Lund University, Lund, Sweden, and the degree of Professor, *honoris causa*, from the Institute for Problems of Information Transmission, Russian Academy of Sciences, Moscow, in 2000.

Since 1976, he has been a faculty member with Lund University where he has the Chair of Information Theory. From 1976 to 2003, he was department Head and during 1988-1993 Dean of the School of Electrical Engineering and Computer Sciences. During 1990-1995, he served as a member of the Swedish Research Council for Engineering Sciences. His scientific interests include information theory, error-correcting codes, and cryptography. In addition to papers in the area of convolutional codes and cryptography, he has authored two textbooks on switching theory and digital design (both in Swedish) and one on information theory (in both Swedish and German) and coauthored *Fundamentals of Convolutional Coding* (New York: IEEE Press, 1999), and *Understanding Information Transmission* (Hoboken, NJ: IEEE Press/Wiley-Interscience, 2005).

Professor Johannesson has been an Associate Editor for the *International Journal of Electronics and Communications*. During 1983-1995 he co-chaired seven Russian-Swedish Workshops, which were the chief interactions between Russian and Western scientists in information theory and coding during the final years of the Cold War. He became an elected member of the Royal Swedish Academy of Engineering Sciences in 2006.

Boris D. Kudryashov was born in Leningrad, U.S.S.R., on July 9, 1952. He received the Diploma in Electrical Engineering in 1974 and the Ph.D in technical sciences degree in 1978 both from the Leningrad Institute of Aerospace Instrumentation, and the Doctor of Science degree in 2005 from Institute of Problems of Information Transmission, Moscow.

In 1978, he became an Assistant Professor and then Associate Professor and Professor in the Leningrad Institute of Aerospace Instrumentation (now the State University on Aerospace Instrumentation, St.-Petersburg, Russia). Since November 2007, he has been a Professor with the State University on Information Technologies, Mechanics and Optics, St.-Petersburg, Russia. His research interests include coding theory, information theory and applications to speech, audio and image coding. He has authored a textbook on information theory (in Russian) and has more than 70 papers published in journals and proceedings of international conferences, 15 U.S. patents and published patent applications in image, speech and audio coding.

Professor Kudryashov served as a member of Organizing Committee of ACCT International Workshops.